Table I. Finite-Field AM1, CPHF 3-21G, and INDO/SDCI results on pNA and TATB[a]

	AM1		3-21G		INDO/SDCI	
	pNA	TATB	pNA	TATB	pNA	TATB
μ_z (D)	-7.64	0.0	-7.79	0.0	-8.34	0.0
$\langle\alpha\rangle$ (Å^3)	11.60	18.90	10.50	16.62	-	-
β_{zzz} (10^{-30} esu)	-11.67	-11.08	-9.55	-8.01	-8.53	-7.68
β_{zyy} (10^{-30} esu)	1.93	11.08	1.66	8.01	0.06	7.68
β_{zxx} (10^{-30} esu)	0.0	0.0	0.0	0.0	0.0	0.0
β_z (10^{-30} esu)	-9.74	0.0	-7.89	0.0	-8.47	0.0
$\|\beta\|$ (10^{-30} esu)	12.14	22.16	9.97	16.02	8.53	15.36

[a] Ground-state dipole moment, μ; average first-order polarizability, $\langle\alpha\rangle$; components of the second-order polarizability tensor; z-component of the vectorial part of the β tensor, β_z; modulus of the β tensor, $\|\beta\|$. Note that β_z is equal to $\sum_i \beta_{zii}$ and $\|\beta\|^2 = \sum_{i,j,k} \beta_{ijk}^2$. The y and z axes define the molecular plane with z corresponding to the para axis (see sketch of the TATB molecule).

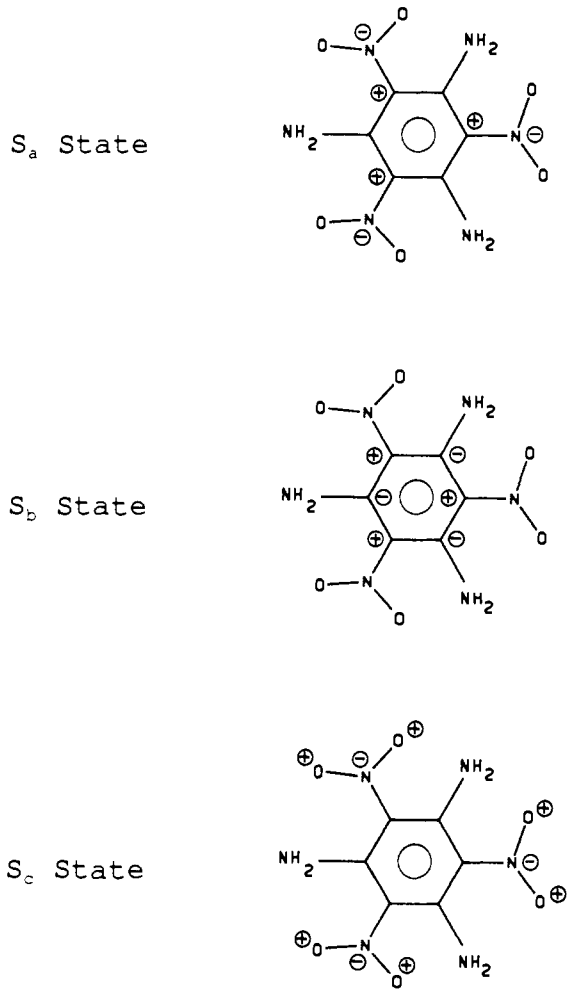

Figure 1. Pictorial representation of the charge transfers in the three excited states which provide the most significant contributions to TATB second-order polarizability. The plus signs (minus signs) represent a decrease (increase) in π-electron charge.

(hereafter denoted S_a, S_b, and S_c states) play an essential role. These states are located 4.64, 5.26, and 6.64 eV above the ground state, respectively.

Relative to the ground state, the charge density evolutions when going to these excited states are illustrated in Figure 1 and correspond to the following: (i) for the S_a state, there occurs a strong polarization of the carbon-nitro nitrogen bonds, with π-electron density transferred from the carbon atom to the nitrogen atom; (ii) for the S_b state, the polarization mostly involves the ring carbon atoms, with π-electron density being transferred from the carbons attached to the nitro groups to those attached to the amino groups; and (iii) in the case of the S_c state, the polarization occurs mainly within the nitro groups with π-electron density moving from the oxygens to the nitrogens. The calculations indicate that the *contributions to β from π-electron transfers between ortho and para pairs of amino and nitro groups are totally mixed and cannot be separated.* Furthermore, as can be seen from the π-electron density evolutions in the essential excited states of TATB, the π-electron densities on the amino groups are found to be less directly involved in the quadratic nonlinear response than is the case in pNA.

Acknowledgment. J.L.B. and F.M. thank SPPS ("Programme Gouvernemental d'Impulsion en Technologie de l'Information", Contract IT/SC/22), FNRS, and IBM-Belgium for the use of the Belgian Supercomputer Network. The work in Mons has been partly supported by the Belgian "Pôle d'Attraction Interuniversitaire: Chimie Supramoléculaire et Catalyse", FRFC, and an IBM Academic Joint Study.

Registry No. pNA, 100-01-6; TATB, 3058-38-6.

Poly(germanium enolate): A New Class of Polymer Having a Germanium Enolate Structure in the Main Chain

Shiro Kobayashi,* Satoru Iwata, Kazuo Yajima, Katsuhiko Yagi, and Shin-ichiro Shoda

Department of Molecular Chemistry and Engineering
Faculty of Engineering, Tohoku University
Aoba, Sendai, 980 Japan

Received January 3, 1992

Polymeric enolates are of great interest from the viewpoints of both basic organic chemistry and material science. The fundamental principle for the generation of a metal enolate from the corresponding carbonyl compound requires an appropriate combination of an electrophilic metallic component M and a nucleophilic component Y.[1] All of the known enolates generated by these methods have monomeric structures because the M-Y bond is cleaved; the production of polymeric enolates cannot be achieved.

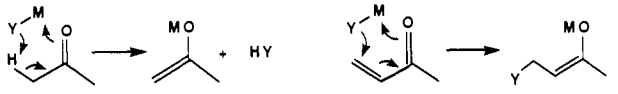

Divalent germanium compounds (germylenes)[2] are interesting chemical species since they have both a nucleophilic center due to the lone pair of electrons and an electrophilic center due to the 4p vacant orbital on the same germanium atom, which enables us to construct a polymeric form of enolate structure. This communication describes the synthesis of novel germanium-containing polymers **3** having a germanium enolate unit in the main chain (*poly(germanium enolate)*) by alternating copolymerization

(1) Typical examples include the preparation of lithium enolates from ketones using lithium amides (M^+ = lithium cation, Y^- = amido anion)[13] and silyl enolate formation from silyl hydrides and α,β-unsaturated carbonyl compounds (M^+ = silyl cation, Y^- = hydride ion).[14]

(2) (a) Rivière, P.; Rivière-Baudet, M.; Satgé, J. Germanium. In *Comprehensive Organometallic Chemistry*; Wilkinson, G., Stone F. G. A., Abel, E. W., Eds.; Pergamon Press: Oxford, **1982**; Vol. 2, pp 399-518. (b) Barrau, J.; Escudié, J.; Satgé, J. *Chem. Rev.* **1990**, *90*, 283. (c) Neumann, W. P. *Chem. Rev.* **1991**, *91*, 311.

0002-7863/92/1514-4929$03.00/0

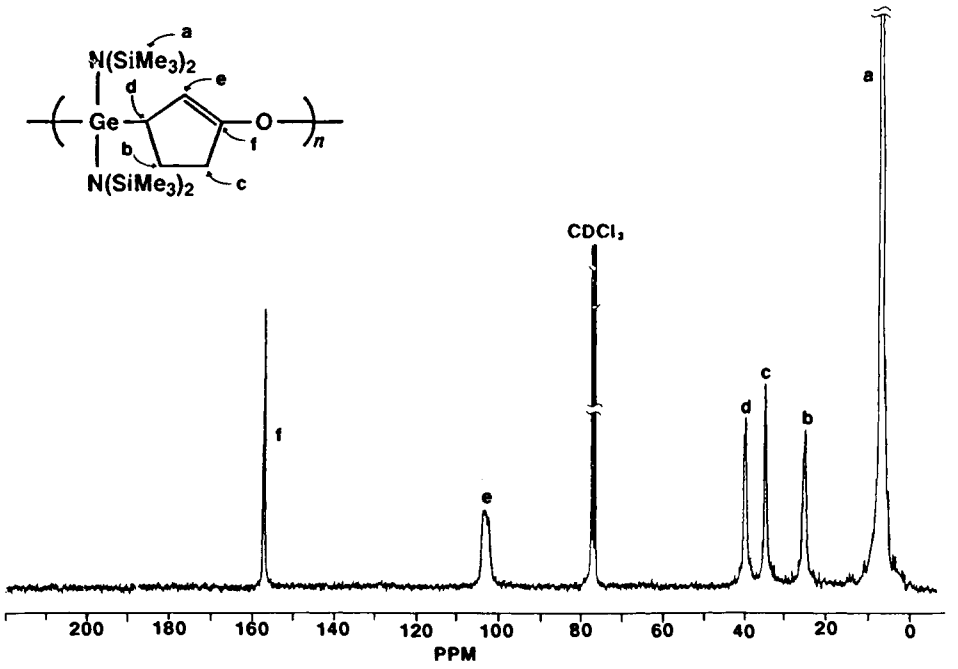

Figure 1. ^{13}C NMR spectrum of copolymer **3a** (entry 2) in $CDCl_3$.

of a divalent germanium compound, bis[bis(trimethylsilyl)-amino]germanium[3] **1**, with cyclic α,β-unsaturated ketones **2**. The resulting polymer **3** is the first example of a metal enolate having a repeating unit structure. The present reaction is a new example of "oxidation–reduction copolymerization", where the germylene is oxidized and the α,β-unsaturated ketone is reduced.[4]

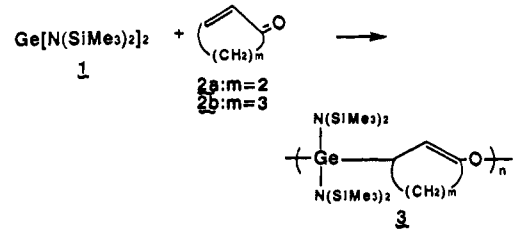

The copolymerization took place smoothly at 0 °C[5] in THF in the presence of a catalytic amount of various lithium compounds, such as lithium bis(trimethylsilyl)amide and *n*-butyllithium (Table I). It is to be noted that a neutral salt (lithium chloride) is also active as catalyst, which allows one to carry out the copolymerization under essentially neutral conditions.[6] In the absence of the lithium salt, no polymerized products were obtained. The copolymerization was complete within 3 h, indicating the high nucleophilic character of **1** toward the carbon–carbon double bonds in α,β-unsaturated carbonyl species.[7] The resulting copolymers[8] are fine white powders and are soluble in common organic solvents such as *n*-hexane and chloroform. The copolymers have high molecular weights ($M_w > 10^5$) and give transparent films by casting. Differential scanning calorimetry (DSC) analysis of the polymer prepared from germylene **1** and 2-cyclopenten-1-one (**2a**) (entry 2) showed a glass transition temperature and a melting point at 40.2 and 220.8 °C, respectively.

Table I. Copolymerization of Germylene **1** with Cyclic α,β-Unsaturated Ketones **2**[a]

entry	copolymer **2**	catalyst	cat. (mol %)	copolymer **3** yield (%)[b]	M_w[c]	M_w/M_N[c]
1	**2a**	none	0	0		
2	**2a**	$LiN(SiMe_3)_2$	0.9	90	4.8×10^5	4.74
3	**2a**	*n*-BuLi	1.0	89	5.2×10^4	2.65
4	**2a**	LiCl	1.0	85	1.1×10^5	2.63
5	**2b**	none	0	0		
6	**2b**	*n*-BuLi	1.0	90	7.6×10^4	2.03
7	**2b**	$LiN(SiMe_3)_2$	1.0	61	4.2×10^5	3.33
8	**2b**	LiCl	1.0	87	3.7×10^5	4.10

[a] Copolymerization was carried out by using 1.2 mmol of **1** and 1.4 mmol of **2** in 3 mL of tetrahydrofuran at 0 °C for 3 h under argon. [b] Isolated yield. [c] Determined by gel permeation chromatography (GPC): eluent, $CHCl_3$; flow rate, 1.0 mL/min; column, Hitachi GL-A130 and GL-A150, polystyrene standard.

The ^1H NMR spectrum of the copolymer obtained from **1** and **2a** (entry 2) exhibited signals which are reasonably assigned to the O-germylated enolate structure.[9] The ^{13}C NMR spectrum of the copolymer shows six peaks at δ 6.3, 25.5, 34.6, 39.7, 103.0, and 157.1 ppm, ascribable to carbon atoms denoted as a–f (Figure 1). These results clearly indicated that a regioselectively O-germylated enolate type polymer **3** was formed: a repeating unit derived from the isomeric C-germylated enolate structure was not detected.

All of the acyclic germanium enolates so far reported are present as C-germylated species **4a** or as a mixture of O- (**4b**) and C-germylated isomers.[10] Therefore, this is the first example of

(3) This compound was prepared according to the following literature. (a) Harris, D. H.; Lappert, W. F. *J. Chem. Soc., Chem. Commun.* **1974**, 895. (b) Gynane, M. J. S.; Harris, D. H.; Lappert, M. F.; Power, P. P.; Rivière, P.; Rivière-Baudet, M. *J. Chem. Soc., Dalton Trans.* **1977**, 2004. (c) Fjeldberg, T.; Haaland, A.; Schilling, B. E. R.; Lappert, M. F.; Thorne, A. J. *J. Chem. Soc., Dalton Trans.* **1986**, 1551.

(4) The new term "oxidation–reduction copolymerization" has been proposed for the alternating copolymerization between germylene **1** and a *p*-benzoquinone derivative in a recent paper. Kobayashi, S.; Iwata, S.; Abe, M.; Shoda, S. *J. Am. Chem. Soc.* **1990**, *112*, 1625.

(5) When the reaction was carried out at a lower temperature (−42 °C), the copolymerization did not take place.

(6) Other metal salts such as lithium fluoride, sodium chloride, potassium chloride, and potassium chloride/18-crown-6 did not produce copolymers effectively.

(7) Similar nucleophilic reactivity of germylene **1** toward carbon–carbon double bonds in acyclic α,β-unsaturated carbonyl compounds has been reported, in which five-membered cyclic germanium enolates were obtained in high yields. Kobayashi, S.; Iwata, S.; Shoda, S. *Chem. Express*, **1989**, *4*, 41.

(8) The copolymers **3** are very stable to moisture. An aqueous THF (95%) solution of **3a** (entry 2) was stirred for 24 h at room temperature. The GPC analysis of the recovered copolymer indicated little change of the molecular weight.

(9) Copolymer **3a** (entry 2): ^1H NMR ($CDCl_3$) δ 0.25 (s, $SiMe_3$, 36 H), 2.30 (br, CH_2CH_2, 4 H), 2.88 (br, GeCH, 1 H), 4.70 (br, =CH, 1 H); IR 1625 cm^{-1} (s, $\nu_{C=C}$). Anal. Found for $(C_{17}H_{42}GeN_2OSi_4)_n$: C, 42.18; H, 9.19; N, 5.69. Calcd: C, 42.94; H, 8.90; N, 5.89.

(10) For example, the formation of germanium(IV) enolates by the reaction of trialkylgermanium chloride and lithium enolates has been reported. (a) Inoue, S.; Sato, Y. *Organometallics* **1987**, *6*, 2568. (b) Lutsenko, I. F.; Baukov, Y. I.; Belavin, I. Y.; Tvorogov, A. N. *J. Organomet. Chem.* **1968**, *14*, 229. (c) Yamamoto, Y.; Hatsuya, S.; Yamada, J. *J. Chem. Soc., Chem. Commun.* **1988**, 1639.

regioselectively O-germylated acyclic enolates[11] which have the potential utility for basic investigation on the stability and nucleophilic reactivity of germanium enolates.

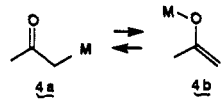

4a 4b

At present, the copolymerization mechanism may be explained as follows. A lithium catalyst reacts with germylene **1** to produce a germyl anion species **5**,[12] to which cyclic ketone **2** adds via a Michael-type addition giving rise to an enolate anion **6**. The germyl anion is regenerated by the reaction of **6** with **1**. The steric hindrance of the bulky silyl amide group of **1** and the very poor homopolymerizability of **2** prevent the homo unit formation of **1** and of **2**, which allows the *alternating propagation* of **1** and **2** leading to copolymer **3**.

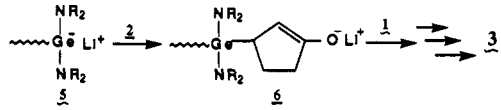

5 6

Further investigations on the physical and chemical properties of the resulting copolymers and the mechanism of the copolymerization are now in progress.

Acknowledgment. This work was partly supported by a Grant-in-Aid for Scientific Research on a Priority Area of "New Functionality Materials, Design, Preparation, and Control" from the Ministry of Education, Science and Culture, Japan (No. 03205009).

(11) The formation of oligomers having a germanium enolate structure by the reaction of difluoro- and phenylhalogermylenes with α,β-unsaturated carbonyl compounds has been claimed; however, the resulting oligomers were not well characterized. Rivière, P.; Satgé, J.; Castel, A. *C. R. Hebd. Seances Acad. Sci., Ser C.* **1977**, *284*, 395.

(12) It is well known that the reaction of a germylene with an alkyllithium affords the corresponding germyl anion.[2] The detailed initiation mechanism is not yet understood.

(13) (a) House, H. O.; Crumrine, C. S.; Teranishi, A. Y.; Olmstead, H. D. *J. Am. Chem. Soc.* **1973**, *95*, 3310. (b) Stork, G.; Kraus, G. A.; Garcia, G. A. *J. Org. Chem.* **1974**, *39*, 3459.

(14) Ojima, I.; Kogure, T. *Organometallics* **1982**, *1*, 1390.

Novel Observation of NH···S(Cys) Hydrogen-Bond-Mediated Scalar Coupling in ^{113}Cd-Substituted Rubredoxin from *Pyrococcus furiosus*

Paul R. Blake,† Jae B. Park,‡ Michael W. W. Adams,*,‡ and Michael F. Summers*,†

Department of Chemistry and Biochemistry University of Maryland Baltimore County Baltimore, Maryland 21228

Department of Biochemistry and Center for Metalloenzyme Studies, University of Georgia Athens, Georgia 30602

Received February 3, 1992
Revised Manuscript Received April 14, 1992

Understanding the nature of NH···S hydrogen bonding in iron–sulfur proteins is important since these interactions may be determinants of protein redox potential and function.[1,2] Very recently, deuteron hyperfine and quadrupole coupling were detected in ^{2}H Mims[3] pulsed ENDOR studies of ferredoxin from *Anabaena*, demonstrating that at least one (unidentified) backbone NH···S hydrogen bond contained significant covalent character.[4] To gain additional insights into the nature of NH···S hydrogen bonding in iron–sulfur proteins, we have applied ^{1}H–^{113}Cd heteronuclear spin-echo difference (HSED) NMR spectroscopy to ^{113}Cd-substituted rubredoxin [^{113}Cd(Rd)] from the hyperthermophilic archaebacterium, *Pyrococcus furiosus* (*P. furiosus*), an organism that grows optimally at 100 °C.[5,6] Of the six backbone NH protons proposed to be involved in NH···S hydrogen bonding,[7-10] four exhibit two-bond N^{1}H···S(Cys)–^{113}Cd scalar coupling, indicating that the NH···S(Cys) hydrogen bonds formed by these protons contain significant covalent character. The ^{1}H–^{113}Cd HSED signals are assigned specifically to the Ile(7), Cys(8), Ile(40), and Cys(41) backbone amide protons that are involved in types I and II NH···S tight turns. No HSED signals are detected for the Tyr(10) and Ala(43) amide protons that are believed to be involved in type II NH···S tight turns. This represents the first NMR observation of H-bond-mediated scalar coupling in a protein and provides a rationale for the high metal affinities exhibited by proteins that contain the Cys-X-X-Cys-Gly-X (X = variable amino acid) metal-binding motif.

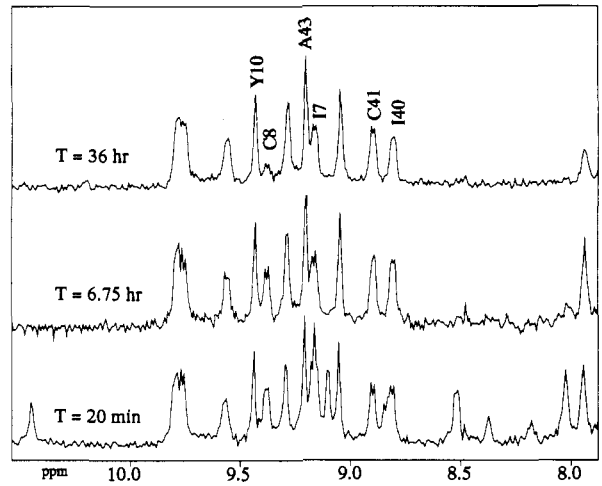

Figure 1. Downfield region of the ^{1}H NMR spectra obtained for Zn(Rd) (ca. 1.2 mM) after dissolution into D_2O at 25 °C. Data were obtained with a GE Omega-PSG 600 NMR instrument using a DANTE sequence for suppression of the residual solvent signal, followed by a SCUBA train for recovery of presaturated αH protons (referenced to internal HDO at δ = 4.773 ppm). Residues implicated in types I, II, and III NH···S hydrogen bonding are labeled.

The NMR structure of zinc-substituted *P. furiosus* Rd [Zn(Rd)] has recently been determined,[9,10] and the structure of the metal-binding site was found to be essentially identical to that observed by X-ray crystallography for native *Clostridium pasteurianum* Rd.[10,11] In both structures the NH protons of residues

* To whom correspondence should be addressed.
† University of Maryland Baltimore County.
‡ University of Georgia.

(1) Backes, G.; Mino, Y.; Loehr, T. M.; Meyer, T. E.; Cusanovich, M. A.; Sweeney, W. V.; Adman, E. T.; Sanders-Loehr, J. *J. Am. Chem. Soc.* **1991**, *113*, 2055.

(2) Sheridan, R. P.; Allen, L. C.; Carger, C. W., Jr. *J. Biol. Chem.* **1981**, *256*, 5052.

(3) Mims refers to a microwave pulse sequence that produces a stimulated electron spin echo: Mims, W. B. *Proc. R. Soc. London, A* **1965**, *283*, 452.

(4) Fan, C.; Kennedy, M. C.; Beinert, H.; Hoffman, B. M. *J. Am. Chem. Soc.* **1992**, *114*, 374.

(5) Fiala, G.; Stetter, K. O. *Arch. Microbiol.* **1986**, *145*, 56.

(6) Adams, M. W. W. *FEMS Microbiol. Rev.* **1990**, *75*, 219.

(7) Adman, E.; Watenpaugh, E. D.; Jensen, L. H. *Proc. Natl. Acad. Sci. U.S.A.* **1975**, *72*, 4854.

(8) Watenpaugh, K. D.; Sieker, L. C.; Jensen, L. H. *J. Mol. Biol.* **1979**, *131*, 509.

(9) Blake, P. R.; Park, J. B.; Bryant, F. O.; Aono, S.; Magnuson, J. K.; Eccleston, E.; Howard, J. B.; Summers, M. F.; Adams, M. W. W. *Biochemistry* **1991**, *30*, 10885.

(10) The high-resolution structure of *P. furiosus* rubredoxin has been determined recently by NMR and X-ray crystallography: Blake, P. R.; Park, J. B.; Zhou, Z. H.; Hare, D. R.; Adams, M. W. W.; Summers, M. F. *Protein Science*, submitted. Day, M. W.; Hsu, E. T.; Joshua-Torr, L.; Zhou, Z. H.; Park, J. B.; Adams, M. W. W.; Rees, D. C. *Protein Science*, submitted.

(11) Superposition of backbone atoms of the metal-binding residues [Cys(5)–Tyr(10) and Cys(38)–Ala(43)] of *P. furiosus* Zn(Rd) onto relevant residues of native *C. pasteruianum* Rd (determined by X-ray crystallography)[7] afforded pairwise RMSD values of ca. 0.33 Å (see ref 10).

0002-7863/92/1514-4931$03.00/0